Journal of Alloys and Compounds, 194 (1993) 295–302
JALCOM 7224

The structure of amorphous binary metal–metal alloys prepared by mechanical alloying*

Christian N. J. Wagner and Michael S. Boldrick
Department of Materials Science and Engineering, University of California, Los Angeles, CA 90024-1595 (USA)

(Received December 9, 1991; in final form June 9, 1992)

Abstract

The structures of amorphous binary metal–metal alloys, prepared by mechanical alloying in a high energy ball mill, can be elucidated by a careful analysis of their neutron and X-ray diffraction patterns, which yield the topological and chemical short-range order. Neutron diffraction studies showed that amorphous Ni_xTi_{100-x} alloys with $24<x<60$ exhibit chemical short-range order, *i.e.* a preference for unlike nearest neighbors. Since V is invisible for neutrons (almost zero scattering length), the neutron structure factor describes directly the atomic arrangement between Ni–Ni and Cu–Cu atoms in amorphous Ni–V and Cu–V alloys. A comparison of the structures of amorphous $Cu_{50}Zr_{50}$ alloys prepared by mechanical alloying, by proton irradiation at low temperatures and by melt spinning showed that their atomic arrangements are very similar. Amorphous alloys of Nb, Ta and W with Fe, Ni and Cu, prepared by mechanical alloying, exhibit atomic arrangements which can be described by a distorted W structure.

1. Introduction

Since the early 1950s, amorphous metal–metal alloys have been prepared by rapid quenching from the liquid or vapor phase in the form of thin foils, ribbons or films. In the past decade, it has been shown that amorphous metallic alloys can also be produced by solid state reactions which include amorphization by hydrogen reaction with intermetallic compounds, interdiffusion in metallic multilayer films, mechanical alloying of metal powder mixtures, mechanical working of intermetallic phases and compounds, and irradiation of intermetallic phases by electrons, protons or ions [1].

The process of mechanical alloying consists of an intimate mixing and mechanical working of elemental powders in a high energy ball or rod mill. This process made it possible to produce amorphous alloys of late transition metals with early transition metals over a much wider concentration range than is possible by liquid quenching, and even in alloy systems which did not yield amorphous phases by rapid quenching from the liquid state [2].

Mechanical working or grinding in a high energy mill is a form of severe plastic deformation at very high strain rates which is responsible for the generation of lattice defects (*e.g.* vacancies, dislocations). It is well known that cold-worked metals and alloys exhibit broad powder pattern peaks. This broadening has been interpreted in terms of the reduction in the size of the coherently diffracting domains (particle, grain or subgrain size) and the appearance of microstrain within these domains [3].

The heavy cold working of the powder in a high energy ball mill decreases the thermodynamic stability of the material because of the generation of lattice defects and the increase in chemical energy due to the increased solubility in solid solutions or the production of antisite defects or antiphase boundaries in ordered phases or compounds. As a consequence, the free energy of the cold-worked crystalline phase might become higher than that of the corresponding amorphous phase, leading to the amorphization of the alloy [1].

In this review, we will summarize the diffraction theory and experiment employed in the evaluation of the structure of amorphous binary metal–metal alloys produced by mechanical alloying. Emphasis will be placed on two special alloy systems, *i.e.* amorphous Ti-base and V-base alloys, where neutron diffraction experiments permit the direct evaluation of one of the three unknown partial atomic distribution functions. We will also compare the structures of amorphous $Cu_{50}Zr_{50}$ alloys prepared by three different techniques: mechanical alloying, liquid quenching and proton ir-

*Paper presented at the Symposium on Solid State Amorphizing Transformations, TMS Fall Meeting, Cincinnati, OH, October 21–24, 1991.

0925-8388/93/$6.00

radiation. Lastly, we will discuss some recent results on mechanically alloyed Nb-, Ta- and W-base alloys.

2. Theoretical background

The atomic short-range order in binary amorphous alloys, consisting of elements of types 1 and 2, is characterized by three atomic pair distribution functions $\rho_{ij}(r)$ describing the number of j-type atoms per unit volume at the distance r about an i-type atom [4], *i.e.* $\rho_{11}(r)$, $\rho_{22}(r)$ and $\rho_{12}(r)$, because $\rho_{21}(r)/c_1 = \rho_{12}(r)/c_2$, c_i being the atomic concentration of element i. An alternative description of the atomic short-range order is given by the number–concentration correlation functions $\rho_{nc}(r)$ [5]. The number–number distribution function $\rho_{nn}(r)$ represents the topological short-range order, responsible for the Bragg peaks in a powder pattern, the concentration–concentration correlation function $\rho_{cc}(r)$ describes the chemical short-range order, and the number–concentration correlation function $\rho_{nc}(r)$ is related to the size difference between atoms 1 and 2 [6]. The functions $\rho_{ij}(r)$ and $\rho_{nc}(r)$ are linearly related, *i.e.*

$$\rho_{nn}(r) = c_1\rho_1(r) + c_2\rho_2(r) \tag{1}$$

$$\rho_{cc}(r) = [c_2\rho_1(r) + c_1\rho_2(r)]\alpha(r) \tag{2}$$

$$\rho_{nc}(r) = c_1c_2[\rho_1(r) - \rho_2(r)] \tag{3}$$

where $\rho_1(r) = \rho_{11}(r) + \rho_{12}(r)$, $\rho_2(r) = \rho_{21}(r) + \rho_{22}(r)$ and $\alpha(r)$ is the generalized Warren short-range order parameter [7] defined as

$$\alpha(r) = 1 - \rho_{12}(r)/c_2[c_2\rho_1(r) + c_1\rho_2(r)]$$
$$= \rho_{cc}(r)/\{\rho_{nn}(r) - [(c_2 - c_1)/c_1c_2]\rho_{nc}(r)\} \tag{4}$$

We define the intensity $S_d(Q)$ scattered by an amorphous or randomly oriented polycrystalline sample as

$$S_d(Q) = I_a(Q) - [\langle f^2\rangle + \langle f\rangle^2\rho_0 V(Q)] \tag{5}$$

where $I_a(Q)$ is the coherently scattered intensity per atom, $\langle f^2\rangle = c_1(f_1)^2 + c_2(f_2)^2$ is the mean square scattering factor, $\langle f\rangle = c_1f_1 + c_2f_2$ is the mean scattering amplitude, and ρ_0 is the average atomic density. The term $\langle f\rangle^2\rho_0 V(Q)$ represents the small-angle scattering, and $V(Q)$ is the Fourier transform of the size function $v(r)$, *i.e.*

$$v(r) = (1/V)\int s(u)s(u+r)\,du$$

where $s(r) = 1$ inside the volume V of the particle and zero outside [4].

The scattered intensity $S_d(Q)$ is the weighted sum of the partial structure factors $S_{nc}(Q)$ which are related to the Fourier transforms of the partial correlation functions $\rho_{nc}(r)$, *i.e.*

$$S_d(Q) = \langle f\rangle^2[S_{nn}(Q) - 1] + (\langle f^2\rangle - \langle f\rangle^2)$$
$$[S_{cc}(Q)/c_1c_2 - 1] + 2\,\Delta f\langle f\rangle S_{nc}(Q) \tag{6}$$

where $\Delta f = f_1 - f_2$. $S_{nn}(Q)$ includes all (hkl) reflections in a powder pattern of nanocrystalline materials, $S_{cc}(Q)/c_1c_2$ describes the modulation of the scattered intensity about the Laue monotonic scattering $\langle f^2\rangle - \langle f\rangle^2$ in binary alloys with short-range order, and $S_{nc}(Q)$ corresponds to the size-effect scattering [6]. The Fourier transforms of $Q[S_{nn}(Q) - 1]$, $Q[S_{cc}(Q)/c_1c_2 - 1]$ and $QS_{nc}(Q)$ yield the number–concentration correlation functions $4\pi r[\rho_{nn}(r) - \rho_0]$, $4\pi r\rho_{cc}(r)$ and $4\pi r\rho_{nc}(r)$ respectively.

The intensity $S_d(Q)$ per atom can also be expressed as the weighted sum of the partial atomic structure factors $I_{ij}(Q)$, *i.e.*

$$S_d(Q) = (c_1f_1)^2[I_{11}(Q) - 1] + (c_2f_2)^2[I_{22}(Q) - 1]$$
$$+ 2c_1f_1c_2f_2[I_{12}(Q) - 1] \tag{7}$$

The Fourier transforms of $Q[I_{ij}(Q) - 1]$ yield the partial reduced atomic distribution functions $G_{ij}(r) = 4\pi r[\rho_{ij}(r)/c_j - \rho_0]$.

In general, the small-angle scattering $\langle f\rangle^2\rho_0 V(Q)$ due to the size of the particles is not observable in amorphous metals, or is subtracted from the scattered intensity. For large values of Q, $I_a(Q) = \langle f^2\rangle$ and $S_d(Q) = 0$. Since $f_i(Q)$ is a slowly decreasing function with increasing Q for X-rays, it is customary to introduce the total structure factors or interference functions $I(Q)$ or $S(Q)$, defined as

$$I(Q) = S_d(Q)/\langle f\rangle^2 + 1 = [I_a(Q) - (\langle f^2\rangle - \langle f\rangle^2)]/\langle f\rangle^2 \tag{8}$$

$$S(Q) = S_d(Q)/\langle f^2\rangle + 1 = I_a(Q)/\langle f^2\rangle \tag{9}$$

The definition of $S(Q)$ has the advantage that it is valid even when $\langle f\rangle^2 = 0$ as is the case for a "zero alloy", an alloy containing the appropriate amount of an element or isotope with negative scattering length for neutrons.

The total structure factors $I(Q)$ or $S(Q)$ permit us to evaluate the reduced atomic distribution functions $G_I(r)$ or $G_S(r)$, *i.e.*

$$G_I(r) = (2/\pi)\int Q[I(Q) - 1]M(Q)\sin Qr\,dQ$$
$$= 4\pi r\{[\rho(r) - \langle f\rangle^2\rho_0]/\langle f\rangle^2\}v(r)$$
$$= \sum_i\sum_j(c_if_ic_jf_j/\langle f\rangle^2)G_{ij}(r)v(r) \tag{10}$$

$$G_S(r) = (2/\pi)\int Q[S(Q) - 1]M(Q)\sin Qr\,dQ$$
$$= 4\pi r\{[\rho(r) - \langle f\rangle^2\rho_0]/\langle f^2\rangle\}v(r)$$
$$= \sum_i\sum_j(c_if_ic_jf_j/\langle f^2\rangle)G_{ij}(r)v(r)$$
$$= 4\pi r\{(\langle f\rangle^2/\langle f^2\rangle)[\rho_{nn}(r) - \rho_0] + (1 - \langle f\rangle^2/\langle f^2\rangle)\rho_{cc}(r)$$
$$+ (2\,\Delta f\,\langle f\rangle/\langle f^2\rangle)\rho_{nc}(r)\}\,v(r) \tag{11}$$

where $\rho(r)$ is the total atomic distribution function, *i.e.*

$$\rho(r) = \sum_i \sum_j c_j f_i c_j f_j \rho_{ij}(r)/c_j \tag{12}$$

and $M(Q)$ is a modification function [3, 4, 8], *e.g.*

$$M(Q) = \sin(\pi Q/Q_{max})/(\pi Q/Q_{max}) \tag{13}$$

or

$$M(Q)\begin{cases} = \exp(-\alpha Q^2) & \text{for } Q < Q_{max} \\ = 0 & \text{for } Q > Q_{max} \end{cases} \tag{14}$$

Q_{max} being the maximum value of the Q range and α an artificial temperature factor, *e.g.* $\alpha = 0.005$.

The total differential correlation function $D(r)$ is given by

$$\begin{aligned} D(r) &= (2/\pi)\int QS_d(Q)M(Q)\sin Qr\, dQ \\ &= \langle f^2\rangle G_S(r) = \langle f\rangle^2 G_I(r) = 4\pi r[\rho(r) - \langle f\rangle^2\rho_0]v(r) \\ &= \sum_i\sum_j 4\pi r[c_j f_i f_j \rho_{ij}(r) - \langle f\rangle^2\rho_0]v(r) \\ &= 4\pi r\{\langle f\rangle^2[\rho_{nn}(r) - \rho_0] + (\langle f^2\rangle - \langle f\rangle^2)\rho_{cc}(r) \\ &\quad + 2\,\Delta f\langle f\rangle\rho_{nc}(r)\}v(r) \end{aligned} \tag{15}$$

The total correlation function $T(r)$ can be deduced from $D(r)$, *i.e.*

$$\begin{aligned} T(r) &= 4\pi r\rho(r)v(r) = 4\pi r\sum_i\sum_j c_i f_i f_j \rho_{ij}(r)\, v(r) \\ &= D(r) + 4\pi r\rho_0\langle f\rangle^2 v(r) \\ &= 4\pi r[\langle f\rangle^2\rho_{nn}(r) + (\langle f^2\rangle - \langle f\rangle^2)\rho_{cc}(r) \\ &\quad + 2\,\Delta f\,\langle f\rangle\rho_{nc}(r)]v(r) \end{aligned} \tag{16}$$

The radial distribution function $R(r)$ describes the number of atoms in the spherical shell of radius r and unit thickness, *i.e.*

$$\begin{aligned} R(r) &= 4\pi r^2[\rho(r)/\langle f\rangle^2]v(r) \\ &= 4\pi r^2\rho_0 v(r) + rG(r) = rT(r)/\langle f\rangle^2 \end{aligned} \tag{17}$$

In amorphous or liquid samples with sizes larger than micrometers it can be assumed that $v(r) = 1$ over the range of r where $\rho(r) - \langle f\rangle^2\rho_0$ is different from zero. This is not true for nanocrystalline or nanoamorphous particles with dimensions of 1–3 nm.

The partial coordination numbers N_{nc} are defined as

$$N_{nc} = \int 4\pi r^2\rho_{nc}(r)m(r)\, dr \tag{18}$$

where $\rho_{nc}(r)$ are defined in eqns. (1)–(3), $m(r) = 1$ for $r \leqslant r_{min}$ and $m(r) = 0$ for $r > r_{min}$, and r_{min} is the r value of the minimum after the first peak in $4\pi r^2\rho_{nn}(r)$.

3. Experimental methods and results

A single diffraction experiment yields only the total structure factors $I(Q)$ (eqn. (8)) and $S(Q)$ (eqn. (9)) which represent the weighted sums of the three partial structure factors $I_{ij}(Q)$ and $S_{nc}(Q)$ respectively. In order to determine the three individual partial structure factors, three diffraction experiments must be carried out, each with a different set of weight factors $c_i f_i c_j f_j$ (eqn. (7)) or $\langle f\rangle^2$ (eqn. (6)). This can be accomplished by preparing three different samples by isomorphous or isotopic substitution of one or both alloying elements. However, there are two special cases in neutron experiments, where a single experiment can yield directly one of the three partial functions. If one of the components has a negative scattering length such as Ti, one can prepare a so-called zero alloy where $\langle f\rangle = 0$, *e.g.* $Ni_{24}Ti_{76}$, which yields directly the concentration–concentration structure factor $S_{cc}(Q)$ (eqns. (6) and (9)), *i.e.* the chemical short-range order. On the contrary, if component element 2 has a zero scattering length, such as V, any alloy consisting of elements 1 and 2 will yield directly the partial structure factor $I_{11}(Q)$ (eqns. (7) and (8)). Therefore, many attempts have been made to prepare amorphous Ti and V alloys by mechanical alloying.

3.1. Amorphous Ti alloys

The production of amorphous Ni–Ti alloys by mechanical alloying was first reported by Schwarz *et al.* [9]. They showed that alloys of Ni_xTi_{100-x} with $25 < x < 75$ will become partially or completely amorphous when appropriate powder mixtures are milled for 24 h in a SPEX 8000 mixer–mill using a hardened steel vial and steel balls under an argon atmosphere. In order to make detailed structural studies by X-ray and neutron diffraction, Boldrick *et al.* [10] prepared amorphous Ni_xTi_{100-x} with $x = 35$, 50 and 60 at.% under the same experimental conditions employed by Schwarz *et al.* [9].

The structure factors $S(Q)$ (eqn. (9)) of the amorphous Ni–Ti alloys are shown in Fig. 1. These factors were deduced from the measured X-ray and neutron diffraction intensities using Ag Kα radiation and an Si solid state detector with the scanning 2θ technique and the time-of-flight method at IPNS Argonne National Laboratory respectively. The scattering lengths f_i of Ni and Ti have the same sign for X-rays, but opposite signs for neutrons, producing strikingly different values of the average scattering amplitude $\langle f\rangle$ for the different Ni–Ti alloys including the so-called zero alloy where $\langle f\rangle = 0$ for neutrons. This difference in $\langle f\rangle$ is strongly reflected in the appearance of the structure factor $S(Q)$ which is dominated by the topological short-range order $S_{nn}(Q)$ in the X-ray data because the weight factor $\langle f\rangle^2/\langle f^2\rangle$ in $S(Q)$ (eqns. (6) and (9)) is 0.986 for all three alloys, but by the chemical short-range order $S_{cc}(Q)$ in the neutron data where $\langle f\rangle^2/\langle f^2\rangle = 0.045$ for

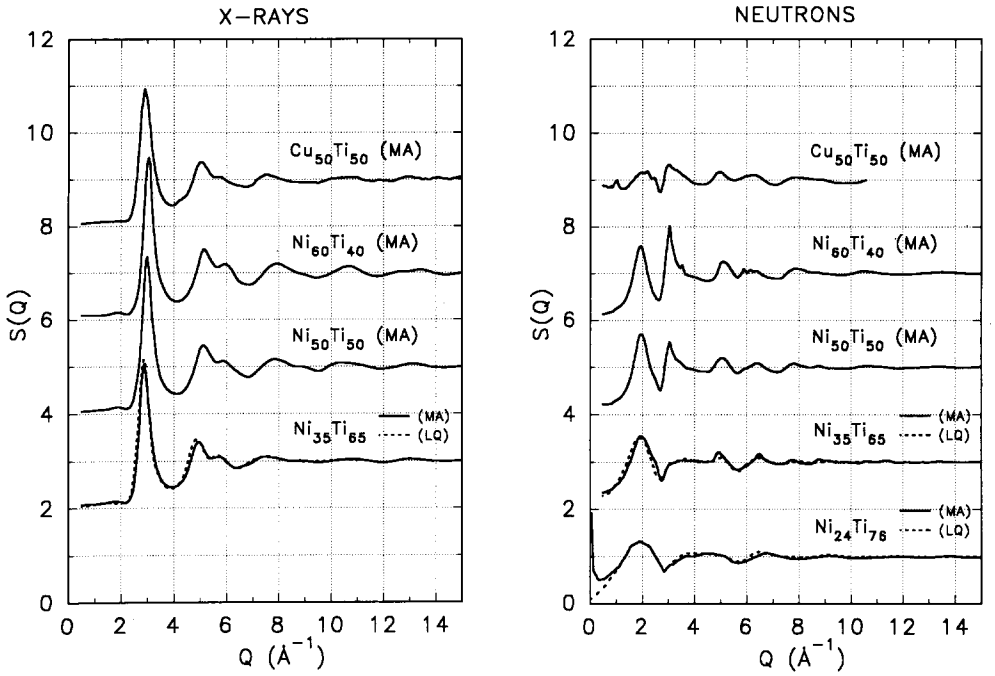

Fig. 1. X-ray and neutron total structure factors $S(Q)$ (eqn. (9)) of amorphous Cu–Ti and Ni–Ti alloys prepared by mechanical alloying and the structure factors $S(Q)$ of the corresponding liquid-quenched alloys (– – –).

the alloy with 35 at.% Ni. Both neutron and X-ray structure factors of the mechanically alloyed $Ni_{35}Ti_{65}$ agree very well with those of the liquid-quenched ribbons (Fig. 1), indicating that their structures are very similar. Fukunaga *et al.* [11] prepared a true zero alloy with the composition $Ni_{24}Ti_{76}$ by mechanical alloying for 800 h in a conventional ball milling apparatus with a rotating speed of 110 rev min^{-1}. The neutron $S(Q)$ is also shown in Fig. 1 and quite similar to that observed in $Ni_{35}Ti_{65}$.

The atomic distribution functions $G_S(r)$ as defined in eqn. (11) are shown in Fig. 2. In the Fourier transformation, all X-ray and neutron structure factors $S(Q)$ measured by Boldrick *et al.* [10] were terminated at $Q_{max}=16$ Å^{-1} and 9 Å^{-1} respectively, using the Lorch function $M(Q)$ given in eqn. (13). The neutron data of Fukunaga *et al.* [11] extended to 30 Å^{-1}. The X-ray $G_s(r)$ which represents largely $G_{nn}(r)=4\pi r[\rho_{nn}(r)-\rho_0]$ exhibits a first peak at $r_1=2.75$ Å in the alloy with 35 at.% Ni. The r_1 values decrease with increasing Ni concentration. The neutron $G_S(r)$ functions are dominated by the chemical short-range order or concentration–concentration correlation function $G_{cc}(r)=4\pi r\rho_{cc}(r)$. As has been observed for the structure factors $S(Q)$, the atomic distribution functions of mechanically alloyed and liquid-quenched samples of identical compositions are quite similar as shown in Fig. 2.

The first negative peak in the alloys with 24 and 35 at.% Ni corresponds to the unlike Ni–Ti nearest neighbors, and combined with the first peak in the X-ray $G_S(r)$ permits the calculation of the generalized Warren short-range order parameter α_1 from $\alpha(r)$ defined in eqn. (4), *i.e.*

$$\alpha_1=\int \alpha(r)m(r)\,dr=N_{cc}/[N_{nn}+N_{nc}(c_2-c_1)/c_1c_2] \qquad (19)$$

In general, the term $N_{nc}(c_2-c_1)/c_1c_2=(c_2-c_1)(N_1-N_2)$ is small when the difference in atomic sizes of the alloying elements is less than 10%, and might be neglected in Ni–Ti alloys. In this case α_1 reduces to the Warren–Cowley short-range order parameter α_{wc} for crystalline alloys. Values of $\alpha_1=-0.15$ and $\alpha_{wc}=-0.10$ were found in the amorphous alloys with 24 at.% Ni and 35 at.% Ni respectively.

Amorphous alloys of Cu–Ti can also be prepared by mechanical alloying [13]. The X-ray and neutron structure factors $S(Q)$ for $Cu_{50}Ti_{50}$, prepared in a SPEX 8000 mill under an argon atmosphere using a hardened steel vial and steel balls [14], are shown in Fig. 1. As has been the case for $Ni_{50}Ti_{50}$, the X-ray pattern is dominated by $S_{nn}(Q)$ whereas the neutron data represent predominantly $S_{cc}(Q)$. More recently neutron diffraction data of amorphous Cu–Ti were obtained by Ivison *et al.* [15] when studying the influence of hydrogen contamination on the amorphization reaction during mechanical alloying. They observed that amorphous alloys could be prepared only in the concentration range 50–75 at.% Cu in hydrogen-free samples by mechanical alloying.

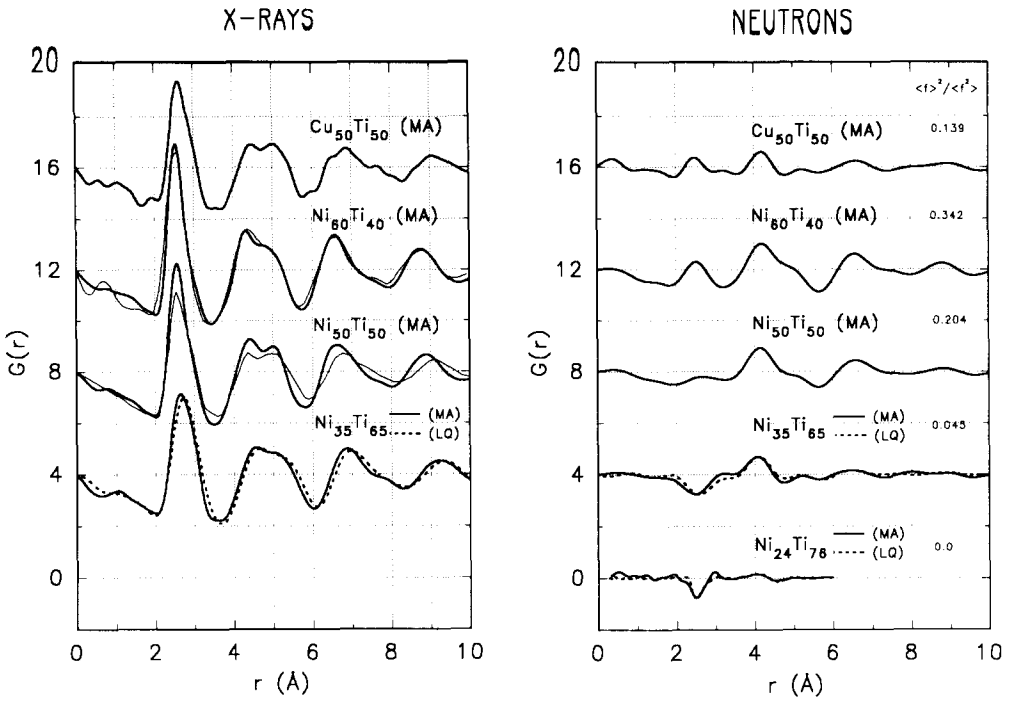

Fig. 2. Total reduced atomic distribution functions $G_S(r)$ (eqn. (11)) of amorphous Cu–Ti and Ni–Ti alloys evaluated from the structure factors in Fig. 1. The light full curves represent the X-ray $G_S(r)$ of $Ni_{60}Ti_{40}$ [9] and $Ni_{50}Ti_{50}$ [12]. $G_S(r)$ for liquid-quenched alloys are also shown (– – –).

3.2. *Amorphous V alloys*

The fact that V has an almost zero scattering length for neutrons was first utilized by Lemarchand *et al.* [16] to determine the partial structure factor $I_{NiNi}(Q)$ in liquid Ni–V alloys. However, no amorphous V alloys have been prepared so far by rapid quenching from the liquid state. Therefore, it was quite a surprise when Fukunaga and coworkers [17, 18] reported the amorphization of Cu–V and Ni–V alloys by mechanical alloying even though the size difference between V and Ni or Cu atoms is only 5%.

The changes in the Cu–Cu partial structure factor $I_{CuCu}(Q)$ and the partial radial distribution function $R_{CuCu}(r) = 4\pi r^2 \rho_{CuCu}(r)/c_{Cu}$ as a function of milling time are shown in Figs. 3 and 4 respectively. After 30 h of mechanical alloying, the $Cu_{50}V_{50}$ alloy has a nanocrystalline structure. All (*hkl*) reflections can be recognized in the maxima of $I_{CuCu}(Q)$, and the face-centered coordination shells are visible in the radial distribution function. After 60 h of milling, the diffraction pattern indicates that the structure of the alloy has become amorphous and it remained unchanged after milling for an additional 60 h. The structure factor and the radial distribution function of the $Cu_{50}V_{50}$ sample, milled for 120 h, are shown in Figs. 3 and 4 respectively. The disappearance of the second and fifth coordination shells, which are found mainly in the octahedral units of the f.c.c. structure, has been used by Fukunaga *et al.* [17] to postulate that the amorphous structure consists mainly of tetrahedral units which are responsible for the third, fourth, sixth and seventh coordination shells and are distinguishable in the amorphous structure.

Similar observations were made by Fukunaga *et al.* [18] during the amorphization of Ni–V alloys. The $Ni_{40}V_{60}$ alloy slowly changes from a nanocrystalline to an amorphous structure with increasing milling time. In addition, they observed that $I_{NiNi}(Q)$ is independent of concentration for the Ni–V alloys with 30–55 at.% Ni, an assumption used by Wagner [4] and his coworkers and Waseda [19] to evaluate the partial functions in liquid alloys.

3.3. *Amorphous Zr alloys*

The amorphization of alloys of Zr with late transition metals by mechanical alloying was first reported by Hellstern and Schultz [20]. A detailed comparison of the structures of amorphous $Cu_{50}Zr_{50}$ prepared by mechanical alloying, melt spinning and proton irradiation was made by Lee *et al.* [21]. The structure factors $I(Q)$ of equiatomic CuZr are shown in Fig. 5 and it is readily visible from the curve which represents the superposition of the three $I(Q)$ that all three CuZr samples possess a similar structure. The same conclusion

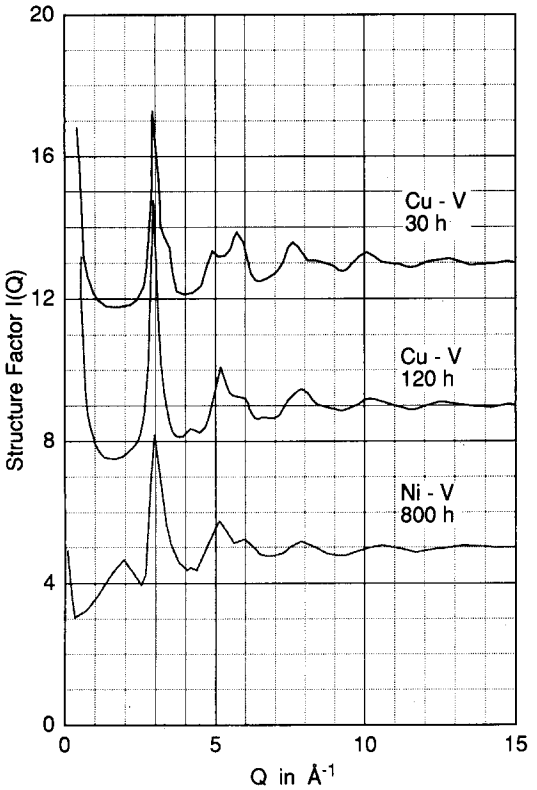

Fig. 3. Neutron structure factors $I(Q)=c_1 I_{11}(Q)$ (eqns. (7) and (8)) of $Cu_{50}V_{50}$ and $Ni_{40}V_{60}$ alloys prepared by mechanical alloying.

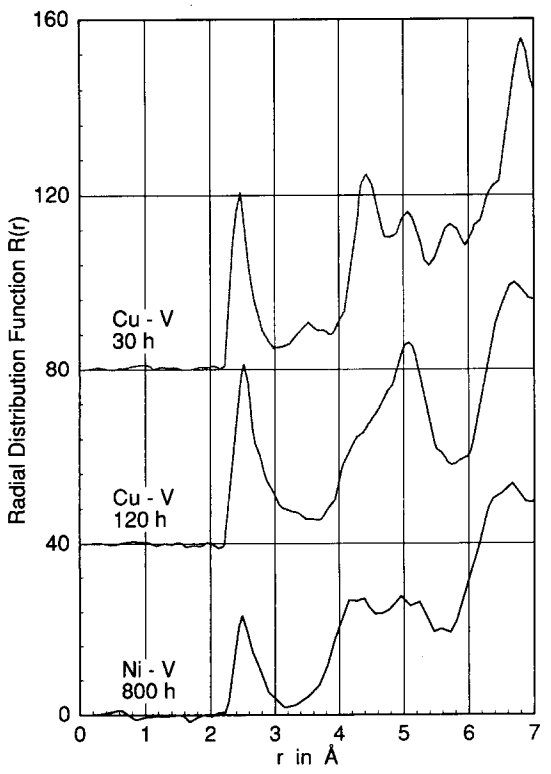

Fig. 4. Neutron radial distribution functions $R(r)$ (eqn. (17)) of amorphous $Cu_{50}V_{50}$ and $Ni_{40}V_{60}$ alloys prepared by mechanical alloying.

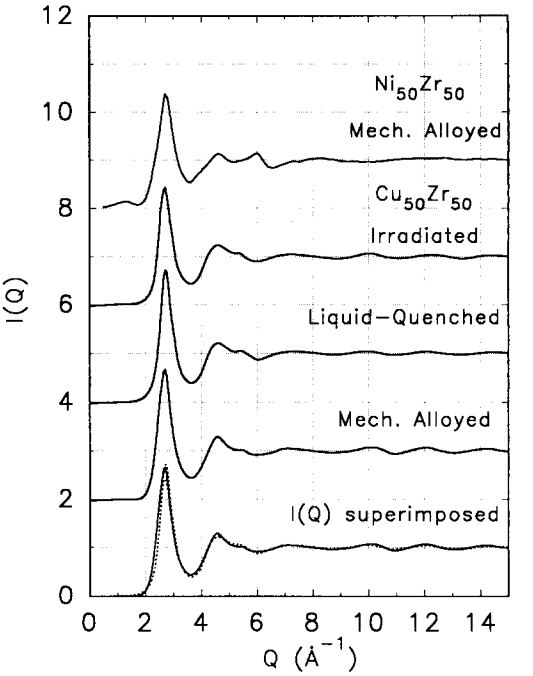

Fig. 5. X-ray total structure factors $I(Q)$ (eqn. (8)) of amorphous $Ni_{50}Zr_{50}$ and $Cu_{50}Zr_{50}$. "$I(Q)$ superimposed" represents the superposition of $I(Q)$ of the irradiated (· · · · ·), liquid-quenched (– – –) and mechanically alloyed (——) samples.

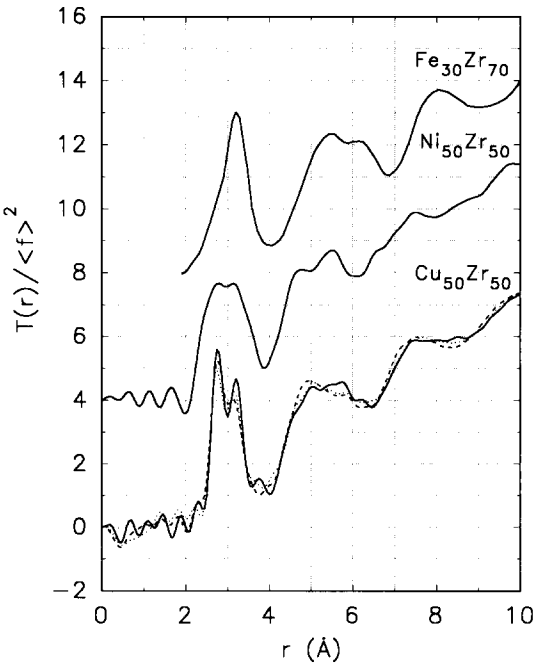

Fig. 6. Total correlation functions $T(r)/\langle f\rangle^2$ (eqn. (16)) of amorphous $Fe_{30}Zr_{70}$ and $Ni_{50}Zr_{50}$ prepared by mechanical alloying. The $Cu_{50}Zr_{50}$ curve represents the superposition of $T(r)/\langle f\rangle^2$ of the irradiated (· · · · ·), liquid-quenched (– – –) and mechanically alloyed (——) samples.

can be drawn from the comparison of the total correlation functions $T(r)/\langle f\rangle^2$ (eqn. (16)) for $Cu_{50}Zr_{50}$ shown in Fig. 6. The splitting of the first peak of $T(r)/$

$\langle f\rangle^2$ with maxima at $r=2.75$ and 3.18 Å is produced by the partial atomic distribution functions $\rho_{CuZr}(r)$ and $\rho_{ZrZr}(r)$. No subsidiary peak is found between 2.5 and 2.6 Å corresponding to Cu–Cu neighbor distances in Cu alloys. It is possible that the weight factor $W_{ij}=c_i f_i c_j f_j/\langle f\rangle^2=0.18$ for the partial function $\rho_{CuCu}(r)/c_{Cu}$ in eqn. (12) is too small to produce a visible subsidiary peak or shoulder on the first peak of $T(r)/\langle f\rangle^2$, or, what is more likely, that the nearest-neighbor distances between Cu–Cu and Cu–Zr atoms are quite similar, producing only one peak at $r=2.75$ Å.

The structure factor of $Ni_{50}Zr_{50}$ is shown in Fig. 5. A small pre-peak at $Q=1.5$ Å^{-1} below the first peak is visible which has been interpreted as evidence for chemical short-range order in amorphous alloys [22]. However, no pre-peak was observed in the X-ray structure factors of liquid-quenched (Ni, Co)–(Zr, Hf) alloys [23]. The correlation function $T(r)/\langle f\rangle^2$ of $Ni_{50}Zr_{50}$ is shown in Fig. 6 which agrees very well with the data of Petzoldt *et al.* [24]. It is qualitatively similar to the corresponding function of $Cu_{50}Zr_{50}$ except that the first peak is broader and exhibits only a small splitting. The correlation function $T(r)/\langle f\rangle^2$ for $Fe_{30}Zr_{70}$ [25], also shown in Fig. 6, is dominated by the Zr–Zr partial function with its maximum at $r=3.16$ Å, identical to the Zr–Zr distances found in amorphous Cu–Zr and Ni–Zr alloys. Using this value for the hard sphere diameter of Zr, Saw and Schwarz [26] have shown that the amorphous Zr alloys such as Ni–Zr can readily be modeled by a dense packing of hard spheres with chemical short-range order, *i.e.* a slight preference for unlike nearest neighbors.

3.4. Amorphous Nb, Ta and W alloys

In contrast to vanadium, the diameters of Nb, Ta, Mo and Ta atoms are much larger than those of Cu, Ni, Fe and Mn, yielding a size difference of 10% or more which constitutes a favorable condition for amorphization. Indeed, the first publication reporting the production of an amorphous alloy by mechanical alloying was by Koch *et al.* [27] on the Ni–Nb system. More recently, it was observed that amorphous alloys can be formed in Cu–Ta [28, 29], Fe–Ta [30], Cu–W [31], Fe–W [32] and Mn–W, Fe–Mo and Mn–Mo [33] by mechanical alloying.

During the process of mechanical grinding of W powder in a high energy ball mill, Boldrick *et al.* [32] observed the formation of an amorphous phase after a 50 h milling time. Chemical analysis by X-ray fluorescence revealed that the milled W powder contained 40 at.% Fe and Cr as a result of the abrasion of the stainless steel balls and the hardened steel vial used in the process. The structure factors $I(Q)$ of the W–Fe alloys are shown in Fig. 7. After 20 h of milling, the alloy containing about 25 at.% Fe and Cr is predominantly nanocrystalline with a particle size of 45 Å and internal strains of 0.5%. By increasing the milling time to 50 h, the Fe and Cr content of the alloy increased to 40 at.%, and the structure of this alloy consists of a mixture of an amorphous phase and a nanocrystalline phase with a particle size of 30 Å. On subtracting the nanocrystalline peaks in the diffraction pattern, we obtained the structure factor of the amorphous $W_{60}Fe_{40}$ alloy shown in Fig. 7, which is dominated by the W–W partial structure factor $I_{WW}(Q)$.

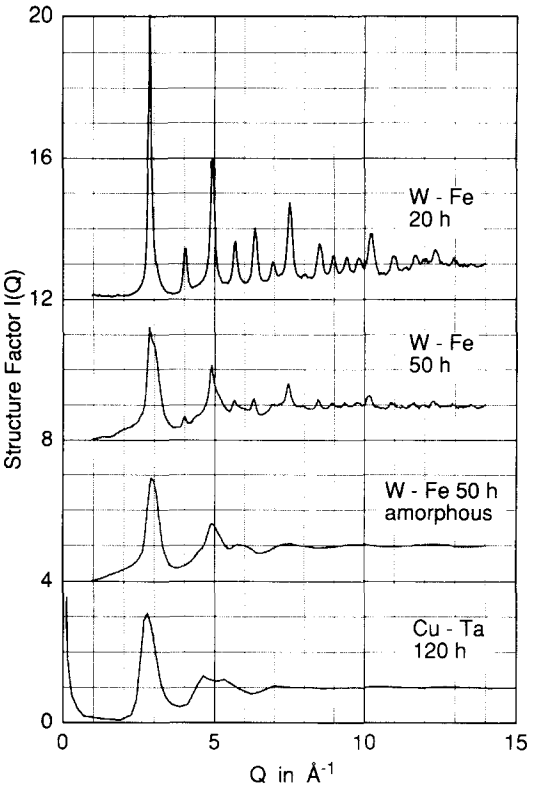

Fig. 7. X-ray total structure factors of mechanically alloyed W–Fe powders milled for 20 h yielding a $W_{76}(Fe, Cr)_{24}$ alloy and milled for 50 h yielding a $W_{60}(Fe, Cr)_{40}$ alloy. Also shown is the neutron total structure factor of amorphous $Cu_{30}Ta_{70}$ [28].

The radial distribution functions $R(r)$ shown in Fig. 8 clearly indicate that the W–Fe alloy milled for 20 h is crystalline with the first coordination shell closely corresponding to that observed in polycrystalline W, *i.e.* $r_1=2.74$ Å. The amorphous $W_{60}Fe_{40}$ alloy possesses a short-range atomic order similar to that found in mechanically alloyed $Ni_{40}Nb_{60}$ [34] and $Cu_{30}Ta_{70}$ [28] also shown in Fig. 8, which can be based on a distorted, more open b.c.c. lattice (W structure) [28].

Neutron scattering experiments revealed that a strong small-angle scattering is present in the structure factors of mechanically alloyed $Ni_{24}Ti_{76}$ [11], $Cu_{50}V_{50}$ [17], $Ni_{40}V_{60}$ [18] and $Cu_{30}Ta_{70}$ [28] as shown in Figs. 1, 3 and 7, clearly indicating that concentration fluctuations extending over a few tens of Ångströms are present in amorphous samples prepared by mechanical alloying.

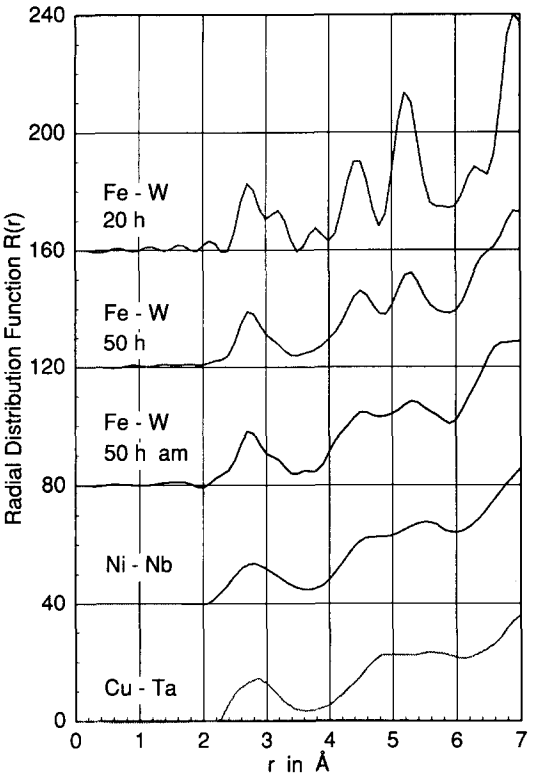

Fig. 8. X-ray radial distribution functions of $W_{76}(Fe, Cr)_{24}$ powders milled for 20 h and $W_{60}(Fe, Cr)_{40}$ powders milled for 50 h. Also shown are the X-ray radial distribution function of the $Ni_{40}Nb_{60}$ alloy [34] and the neutron radial distribution function of the $Cu_{30}Ta_{70}$ alloy [28].

Such fluctuations are absent in the liquid-quenched $Ni_{24}Ti_{76}$ alloy, as shown in Fig. 1.

Acknowledgments

Part of the research reported in this review was supported by the National Science Foundation under Grant DMR 89-10892 and also benefited from the use of the Pulsed Neutron Source at Argonne National Laboratory.

References

1 W. L. Johnson, *Mater. Sci. Eng., 97* (1988) 1.
2 A. W. Weeber and H. Bakker, *Physica B, 153* (1988) 93.
3 B. E. Warren, *X-Ray Diffraction,* Addison-Wesley, Reading, MA, 1968.
4 C. N. J. Wagner, in S. Z. Beer (ed.), *Liquid Metals, Chemistry and Physics,* Dekker, New York, 1972, p. 257.
5 A. B. Bhatia and D. E. Thornton, *Phys. Rev. B, 2* (1970) 3004.
6 A. C. Wright and C. N. J. Wagner, *J. Non-Cryst. Solids, 106* (1988) 85.
7 C. N. J. Wagner, *J. Non-Cryst. Solids, 31* (1978) 1.
8 E. A. Lorch, *J. Phys. C, 2* (1969) 224.
9 R. B. Schwarz, R. R. Petrich and C. K. Saw, *J. Non-Cryst. Solids, 76* (1985) 281.
10 M. S. Boldrick, D. Lee and C. N. J. Wagner, *J. Non-Cryst. Solids, 106* (1988) 60.
11 T. Fukunaga, M. Misawa, K. Suzuki and U. Mizutani, *Mater Sci. Forum,* (1991), to be published.
12 S. Enzo, L. Schiffini, L. Battezzati and G. Cocco, *J. Less-Common Met., 140* (1988) 129.
13 C. Politis and W L. Johnson, *J. Appl. Phys., 60* (1986) 1147.
14 M. S. Boldrick and C. N. J. Wagner, *Mater. Sci. Eng., A 134* (1991) 872.
15 P. K. Ivison, N. Cowlam, I. Soletta, G. Cocco, S. Enzo and L. Battezzati, *Mater. Sci. Eng., A 134* (1991) 859.
16 J. L. Lemarchand, J. Bletry and P. Desre, *J. Phys. (Paris), Colloq. C8, 41* (1980) 163.
17 T. Fukunaga, M. Mori, K. Inou and U. Mizutani, *Mater Sci. Eng., A 134* (1991) 863.
18 T. Fukunaga, V. Homma, K. Suzuki and M. Misawa, *Mater. Sci. Eng., A 134* (1991) 987.
19 Y. Waseda, *The Structure of Non-Crystalline Materials,* McGraw-Hill, New York, 1980.
20 E. Hellstern and L. Schultz, *Appl. Phys. Lett., 48* (1986) 124.
21 D. Lee, J. Cheng, M. Yuan, C. N. J. Wagner and A. J. Ardell, *J. Appl. Phys., 64* (1988) 4772.
22 H. Ruppersberg, D. Lee and C. N. J. Wagner, *J. Phys. F, 10* (1980) 1645.
23 D. Lee, A. Lee, C. N. J. Wagner, L. E. Tanner and A. Soper, *J. Phys. (Paris), Colloq. C9, 43* (1982) 19.
24 F. Petzoldt, B. Scholz and H. D. Kunze, *Mater. Sci. Eng., 97* (1988) 25.
25 W. Biegel, H. U. Krebs, C. Michaelsen, H. C. Freyhardt and E. Hellstern, *Mater. Sci. Eng., 97* (1988) 59.
26 C. K. Saw and R. B. Schwarz, *J. Less-Common Met., 140* (1988) 385.
27 C. C. Koch, O. B. Cavin, C. G. McKamey and J. O. Scarbrough, *Appl. Phys. Lett., 43* (1983) 1017.
28 C. H. Lee, M. Mori, T. Fukunaga, K. Suzuki and M. Mizutani, *Mater. Sci. Forum,* to be published.
29 G. Veltl, B. Scholz and H. D. Kunze, *Mater. Sci. Eng., A 134* (1991) 1410.
30 T. Fukunaga, K. Nakamura, K. Suzuki and U. Mizutani, *J. Non-Cryst. Solids, 117–118* (1990) 700.
31 E. Gaffet, C. Louison, M. Harmelin and F. Faudot, *Mater. Sci. Eng., A 134* (1991) 1380.
32 M. S. Boldrick and C. N. J. Wagner, *J. Non-Cryst. Solids, 150* (1992) 478.
33 E. Yang, C. N. J. Wagner and M. S. Boldrick, *Proc. 3rd Int. Conf. on Amorphous Materials, Topolcianky Castle, Czechoslovakia, September, 1992.*
34 F. Petzoldt, *J. Less-Common Met., 140* (1988) 85.